Journal of Structural Dynamics

A Novel Approach For Measuring The Vibration Properties Of Non-Metallic Materials

Shabarish Sriraman*[1], Hugh Goyder[2]

[1] *Atomic Weapons Establishment, Aldermaston, Reading, Berkshire, RG74PR, U.K.*
[2] *Centre for Defence Engineering, Cranfield University, Defence Academy of the United Kingdom, Shrivenham, SN68LA, U.K.*

Abstract

Non-metallic materials display frequency and temperature dependent dynamic properties which must be characterised for use in computer simulations. The characterisation of such properties is important as most modern structures utilise these materials. Hence, a novel test method has been developed, which combines vibration testing with finite element analysis, to yield dynamic modulus of elasticity and damping. Material properties have been measured in the frequency range 2Hz - 2000Hz.

The test method involves a cantilever beam. Two samples of the test material sandwich the root of the beam and are held in place between inertial masses. Experimental modal analysis techniques, where an instrumented hammer vibrates the beam, are used to exercise the material. The modulus of elasticity of the material is found by constructing a finite element model of the test setup and tuning the simulated response with that of the experiment. Damping properties are extracted by applying data fitting techniques to the time histories and spectrum. These are then converted into a material damping property by simulating and accounting for the energy balance between the samples and test setup. Doing so also improves damping simulation accuracy by eliminating the need to estimate Rayleigh damping values at each frequency, as now the material damping property at each frequency can be directly used.

For test accuracy, it is important that the sample is gripped in a manner that exercises it effectively and is simple to simulate. Eliminating slipping, and thus the difficult to model friction, is a key concern and has been investigated in depth. The best solution found is an axisymmetric bolting arrangement which holds the samples in place. Additionally, the test setup utilises suspension, together with inertial masses and an orthogonal layout to isolate against external vibrations.

Polymers and rubbers, which exhibit complex frequency dependent behaviour, have been reliably characterised using this method. The damping material Sorbothane has also been re-characterised and produced results that aligned with manufacturer specifications. This method proves to be a reliable procedure for dynamic material property testing.

Keywords: Non-metallic materials, High frequency testing, Property characterisation method, Damping quantification, Interface stress distribution, Material joints, Non-linear response

Received on June 24, 2024, *Accepted on March 24, 2025*, *Published on April 7, 2025*

1 Introduction

Modern structures are composed of several different materials and predicting their vibrational response with theoretical methods becomes impossible when the underlying material properties are unknown. The major trend in engineering is to incorporate more non-metallic materials in designs due to their favourable environmental and efficiency impacts. Aircraft design exemplifies this trend well, as in the span of just 25 years, airframe structures are now made up of 52% more composites [1].

Built-up structures spanning nearly every industry must contend with vibrations, and as the materials used heavily determine their dynamic response, the two are invariably linked. The key properties that influence a material's vibration

*Shabarish.Sriraman@awe.co.uk

response are its Young's modulus and damping characteristics. Several novel materials display frequency and temperature dependant vibration properties. Thus, to maintain satisfactory behaviour of a structure over its full operational envelope, comprehensive characterisation is required. Material property data is also the primary input into the simulation process, which itself is integral in engineering design.

This paper sets out a novel method for material characterisation which overcomes key restrictions in current approaches. Notably:

- Both Young's Modulus and damping properties can be measured
- A wide frequency range can be characterised (2-2000Hz)
- The allowable geometry of potential samples is versatile
- Sample gripping is well defined and verified using simulation
- Significant insulation from external vibration sources is achieved
- Sample excitation is largely uniform throughout the frequency range
- Properties are evaluated quickly and the method remains inexpensive

Currently, the process for characterising materials for use in simulation often involves consulting with an external company. This is expensive and time consuming [2], often taking several weeks for turnaround, and hence creates a disconnect in the engineering design process. Even if the required equipment is on hand, specialist staff need to be trained, adding further inefficiency.

The vibrational properties of materials are most often characterised using a dynamic mechanical analysis (DMA) machine. These work by applying a sinusoidal displacement at a desired frequency and measuring the resulting strain in the material sample [3]. However, these machines are limited by the frequency ranges they offer, often reaching their high frequency limit at 200Hz [4]. High frequency DMA solutions do exist, such as the VHF 104 [5], which extend the frequency range up to 10kHz. However, such approaches use extrapolation to reach higher frequencies and are prone to significant shaker-structure interactions where the properties of the excitation column become entangled with the properties of the sample under test. In cases of material characterisation, absolute properties are required as any extrapolation is underpinned by its assumptions. Notably, time temperature superposition is often used to synthetically extend the reported range for polymeric materials. However, for this assumption to apply, the material must be homogeneous, isotropic, amorphous and most importantly, linear viscoelastic in the full region of interest. Additionally, in polymers with a range of activation energies or complex relaxation processes, the linear assumption does not hold [6].

Being able to extend the testable range is important as many, especially viscoelastic, materials display frequency dependant behaviour [7]. Further, many engineering applications, ranging from jet engine combustion [8] to undersea petrochemical piping [9] display resonant modes at frequencies beyond the scope of traditional methods. In cases where alternative, laboratory-based characterisation methods are used [10], the influence of external vibrations may not be fully considered. Additionally, the use of an external shaker to excite the sample [11] shaker-structure interaction. These corrupt measured results by adding the shaker's stiffness and damping properties to that of the sample [12], in a similar manner with the excitation columns of DMA machines.

Characterisation results are also dependant on sample size and shape [13]. Samples may need to be carefully machined to match the clamping arrangement, which may not always be possible for new materials with property or production constraints. This is especially true in cases where the sample is required to be a vibrating beam [14].

The manner in which samples are gripped is important to avoid slippage and the difficulties associated with friction. Material samples undergoing characterisation are commonly held in place using grips. Dynamic Mechanical Analysis (DMA) machines offer multiple grips to hold samples [15]. As slippage during testing invalidates dynamic property characterisation, manufacturers have considered several different clamping types [16]. Mucsi in 2013 [17], developed and evaluated a novel gripping system that self-aligns to ensure uniaxial conditions. Despite this, Anssari-Benam et al. in 2012 [18] bring forth the issue with using grips by highlighting the Saint Venant's principle. Specifically, the distance between the location of material being held and the material under test is often too small to discount the impact of the holding mechanism. Love et al. in 1944 [19] demonstrated that using teeth-based gripping mechanisms result in irregular strain field distributions near the gripping points which decay with distance. This distance is referred to as the characteristic decay length [20] and within it, sample behaviour is irregular. Beyond this length, the influence of the gripping points is diminished, and sample behaviour returns to expected behaviour. Sönnerlind in 2018 [21] considered the impact of the Saint-Venant's principle within a simulation environment. Sample material within the characteristic decay length produced unreliable results, which is not suitable when characterising a material. Further, characteristic decay length is material dependent and varies greatly, for example, graphite/epoxy composites have characteristic lengths four times greater than isotropic metals [22]. Thus, either the influence of any gripping points must be accounted for, or a gripping arrangement which uniformly holds the sample is required. Sample gripping has been investigated in detail as part of the proposed characterisation method.

Simulating damping using the finite element method poses further challenges. Rayleigh damping is commonly used, which uses two parameters to cover the entire frequency range - one parameter scaling with mass and the other with stiffness [23]. However, damping ratio and stiffness values are required for each vibration mode to begin to represent material properties correctly, and full damping representation requires a matrix of these values. Thus, due to lack of measured data and complexity of representation, comprehensive material characterisation may not be possible. This leads to the necessity of assumptions and estimations being used which lowers the accuracy of simulated damping [24].

In this paper, a method for reliably characterising a material's modulus of elasticity and damping properties is presented. Material examples from multiple different families (metals, polymers and rubbers) have been tested and validated against expected values. An existing, well characterised, viscoelastic damping material has also been retested using this method. The next section details the method setup and measurement procedure. This is followed by a detailed investigation into the sample gripping arrangement. A section then gives examples of measured results. The proposed method is then evaluated considering the results and concludes with closing remarks presented.

2 Test Setup

A quasi-cantilever beam is used to exercise the material samples. Two samples are used: one on either side of the root of the cantilever. The dimensions of the beam are selected to produce a large number of distinct modes (typically about 11) in the desired frequency range of 2-2000Hz. This frequency range was chosen as it covers a significant number of engineering applications. If greater resolution is required in a different frequency band, the beam length, thickness or material may be altered. Variable thickness beams have also been investigated as part of this work and show promise in further resolution refinement. Alternatively, a tip mass may be added to augment beam characteristics. Figure 1 shows an overhead view of the setup.

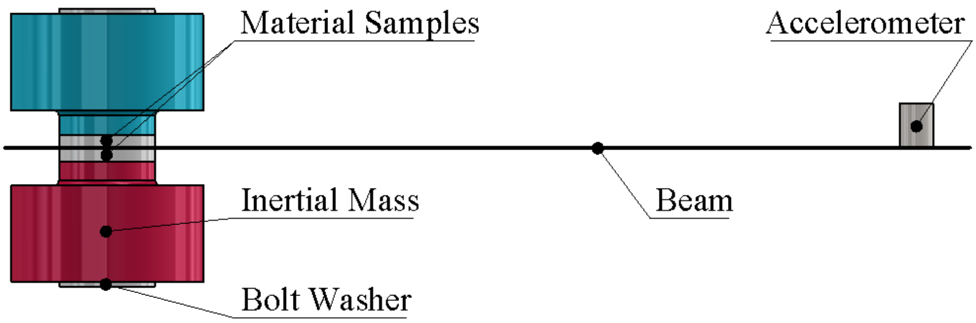

Figure 1: Schematic Diagram of Test Setup

As noise free measurements are desirable, insulation from external vibrations is important. Thus, the test setup is suspended from an external frame using a thin inelastic rope to reduce the transmission of ground vibrations. The primary vibrating axis of the beam is also orthogonal to the suspension to eliminate any remaining suspension interference. Additionally, inertial masses sandwich the beam-samples setup and act as the mounting points for the suspension. This ensures that any final interfering vibrations are negligible. Figure 2 shows these concepts. Additional experiments were also done to verify this. The sensitivity of the dynamics of the rig to force excitation angle was tested using an electromagnetic excitation rig and was found to have negligible impact. Additionally, as ten runs are taken per sample and the extracted natural frequencies are averaged, the impact of occasional force misalignments is minimized. Furthermore, the influence of the accelerometer cable mass impacting rig dynamics was also negated by using an additional suspension loop which supports the weight of the cable.

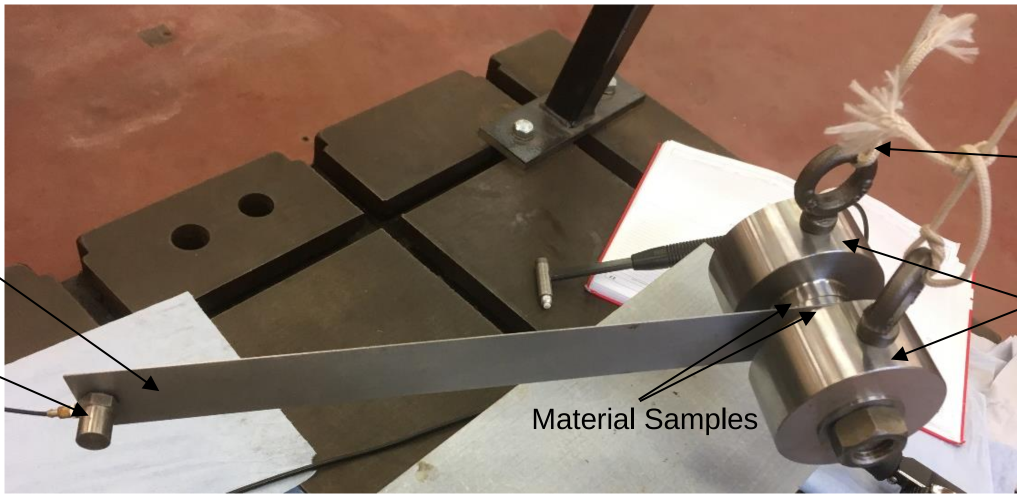

Figure 2: Picture of Test Setup

3 Investigation Of Sample Gripping

The initial design philosophy of the method used rectangular samples to cater for geometries of varying lengths and thus enabled greater flexibility in sample dimensions. This is important as some materials, such as soft rubbers or more brittle materials, may be difficult to machine into more intricate shapes. As a result, samples would often be a fraction of the entire length of the inertial mass and are referred to as “short samples” in this section. The four holes shown on the inertial mass surface represent the studding locations and thus the regions from which the clamping force originates.

Quasi static simulations were used to assess the stress distributions cross the face of the sample. Importantly, the bolt torque and the resulting preload, was varied in the model in line with values suggested in international standards. This expectedly changed the magnitude of results but not the distribution. Frictional contacts, using values of dynamic friction from literature where possible, such as 0.3 for steel-on-steel contact [25], were defined between material boundaries. From this, the principle and von Mises stress distribution across the face of the sample was calculated. Von Mises plots are shown as these incorporate the shear stress that arise from Poisson effects in the softer materials. For small strains, the principle stress and von Mises stress are essentially identical, and represent the contact pressure of the interface.

Simulating the static loading of this configuration, as shown in the stress plot in Figure 3, demonstrates the key drawback of using short samples. Despite the studding points being symmetrically spaced, each point in the sample is unequally distant to these points. In these diagrams, the green and yellow regions represent relatively high stress, and the blue regions represent relatively low stress. Thus, a uniform stress distribution would be represented by a singular colour, usually aquamarine, as fewer disparities are present. Using this, the regions of the sample nearest to these studding points experience the most stress (as indicated by the green and yellow zones) and are held in place well. However,

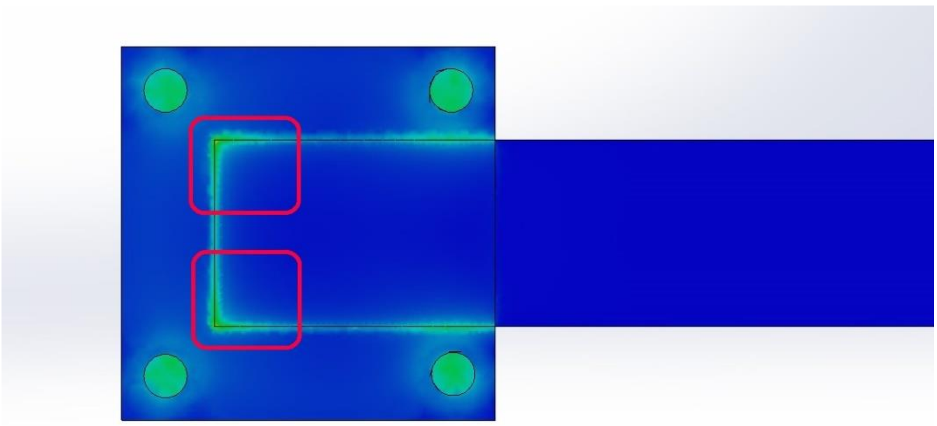

Figure 3: Static Loading of Short Samples

central parts of the sample edges are less well stressed, as shown by the blue stress region. Further, due to the samples being shorter than the full length of the inertial mass, a greater moment on the region of sample further away from the edge is experienced.

Figure 4 helps convey the significant change in sample gripping by comparing short and long samples. The normal stress distribution across the face of the sample in direct contact with the beam, under typical static loading conditions used during testing, is plotted. The increased stress on the edge of the short sample near the root of the beam, resulting from the asymmetrical loading and moment generation, is displayed on the top figure. On the lower figure, the edge gripping all around the full-length sample is evident, which clearly indicates a more thorough gripping definition. The rectangular samples rig helped identify the importance of careful engineering of the material sample gripping profile. A dual axis of symmetry loading arrangement was established by moving away from samples of varying lengths, to full length samples. This enabled a symmetrical, but non-uniform, gripping distribution over just the edges. The key assumption here is that if a sample is well gripped on all its edges, then its centre is well gripped too. Though this may be a valid assumption for relatively stiff materials, the method is designed to offer capability when testing softer materials as well. Thus, methods of improving gripping in the centre of the sample were explored.

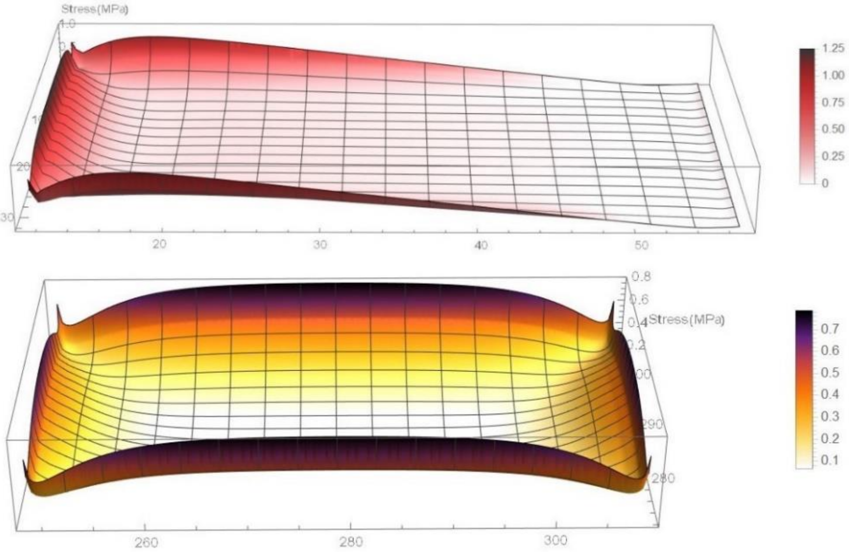

Figure 4: Normal Stress Distribution Across Short (Top) & Full (Bottom) Sample

3.1 Edge Grips Study

Edges represent areas of significant gripping stress. Hence, a discrete edge grip, which would be attached between the inertial mass, the sample and the beam, was designed to introduce edges to the central regions of the material sample. The grip is placed between each layer to ensure the centre of the material is well gripped on either side of the sample. As can be seen from the stress regions in Figure 5, the additional edges on the narrow spokes are well defined in the static loading simulation. Additionally, the outside edges of the sample, especially those nearest to the loading points, remain as the most well gripped regions, shown by the yellow and bright green colours, as opposed to the turquoise colours on the spokes.

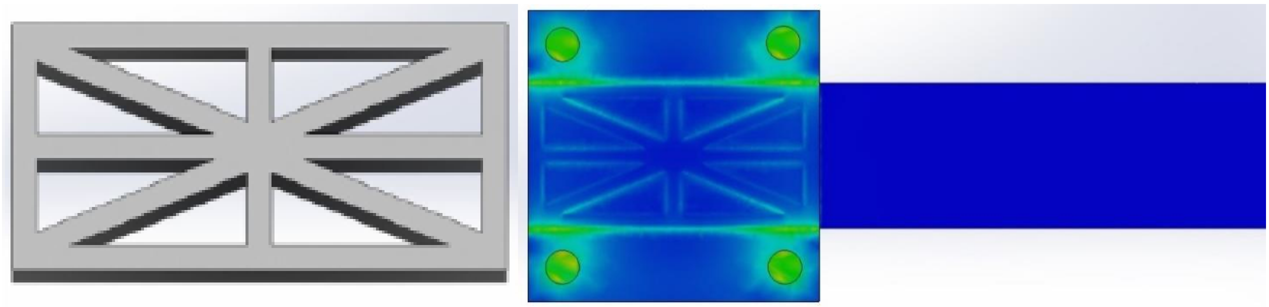

Figure 5: Edge Grips Study Grip Design (Left) & Resulting Stress Distribution (Right)

3.2 Washer Grips Study

As a result of the impact edges play in enhancing sample gripping, circular washer grips were prototyped. The rationale behind this geometry is the internal edge provided by the central hole. Further, circular samples would ensure uniform loading over the entire edge. Two washer designs, with varying internal to external diameter ratios, were modelled to observe the impact of changing the size of the hole on sample stress distribution. Figure 6 compares the narrow and wide washer grip designs under a static load. The narrow washer produces a very well defined and uniform stress distribution on both the internal and external edges. However, despite the same being true for the wider washer samples on the external edge, there is a clear decay in stress from the external to the internal edge. This is noteworthy as it indicates the need to find the optimal internal/external radii ratio, which maintains uniform loading while maximising the region of sample material being gripped. The latter is important to ensure enough of the sample is exercised to influence system behaviour. In order to maximise the sample material being exercised, the next step was to use multiple narrow washers positioned across both sides of the sample. This produced region of well-defined gripping as clear indents of the internal and external edges were left in the samples and the beam.

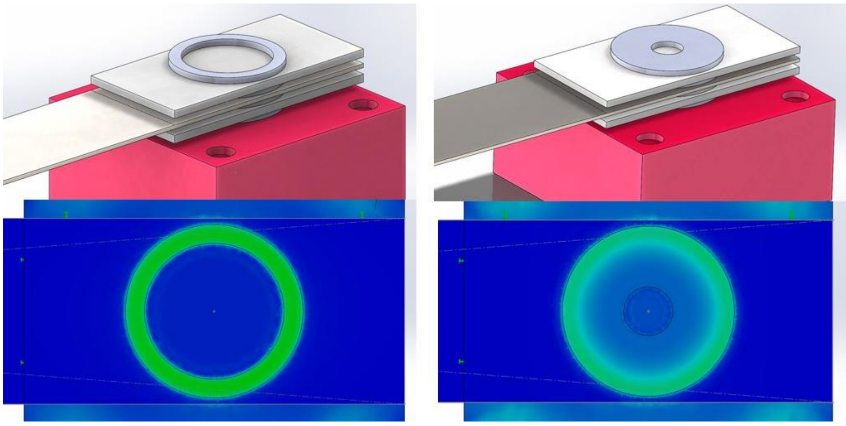

Figure 6: Narrow vs Wide Washer Grips

Despite this, these indented zones represent the same issues as using traditional teeth-based grips, as is the case in current DMA approaches. This is because a variable strain field is applied around each washer, the impact of which is difficult to determine. Furthermore, the nature of the strain field varies with each material sample, and thus proves problematic when simulation simplicity and characterisation accuracy are key objectives. Assembly too becomes arduous, as each interface, of which there are four, requires multiple washers, each to be positioned and remain steady when clamping down the rig. The precise placement of each washer is necessary to ensure uniform loading and validating this positioning for each assembly adds significantly to the overall test length. Even if the beam and inertial masses had these washer patterns engraved into their surfaces, which once again increases simulation complexity, doing so would significantly increase the precision manufacturing capability required and potentially make the design inaccessible to some in-house testing. Thus, a sample holding method which does not introduce indents, and thus the resulting variable strain fields, is required for material characterisation.

3.3 Radii Ratio Study

The washer grip tests unveiled the potential behind using circular samples with a central hole. As the ratio between the internal (IR) and external (ER) edges was found to be critical in the observed stress distribution between the two edges, this behaviour was investigated further. Hence, cylindrical material samples with varying IR/ER ratios were modelled and simulated. It is important to add that the inertial masses have been remodelled to match the circular cross section of the sample at the contact interface. A static load, similar to the clamping force experienced by the samples during testing, is applied to the mass-sample-beam-sample-mass sandwich arrangement to observe changes in the stress distribution throughout the material. Figure 7 compares the results obtained from this study and demonstrates the following three significant results, which remain consistent with varying levels of mesh refinement:

- If the radii ratio is too large (0.9 and 0.65 in the figure), i.e. the hole is too large, the sample experiences high stress on the internal edge.
- If the radii ratio is too small (0.3 and 0.1 in the figure), i.e. the hole is too small, the sample experiences high stress on the external edge.

- An ideal radii ratio was found where the stress distribution remains uniform throughout the face of the entire sample (0.53 in the figure).

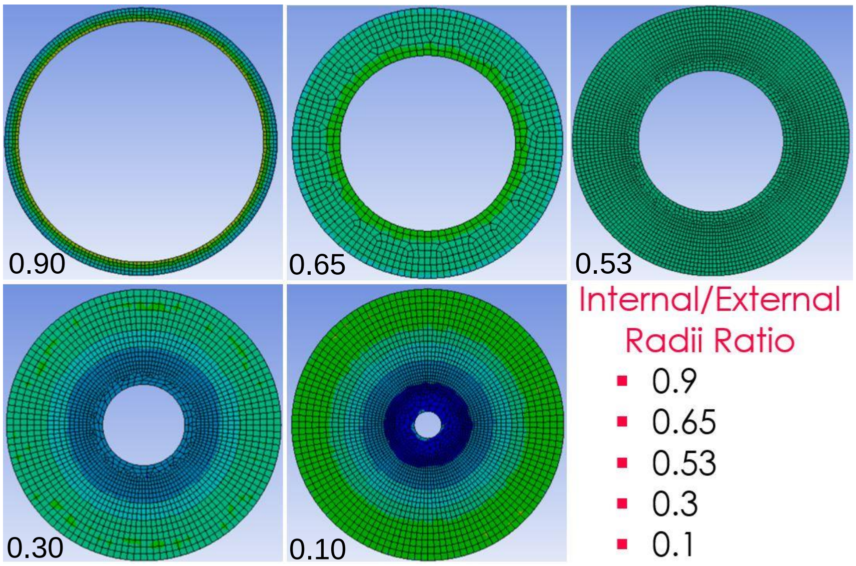

Figure 7: Radii Ratio Study - Mild Steel

This is a significant finding as it highlights the variability of sample gripping with geometry. The disproportionate nature arising from one edge being gripped especially well also opens the possibility of gapping behaviour, where the surfaces of the sample and the test apparatus may separate. It is also important to note that these results used mild steel as the sample and rig material. To compare how stress distribution changes with sample material, rubber samples were also simulated.

Figure 8 displays the stress distributions observed for the rubber samples under the same loading arrangement. Rubber's stress distribution differs markedly from the mild steel, in that every geometry tested shows notable stresses on both the inside and outside edges. Even when comparing between the extreme cases in geometry (0.9 vs 0.1), a high stress, green-yellow, region is present on the edges and a low stress, blue, region is present between the edges. Changing geometry only changes the decay in stress from the edge. In the 0.9 case, this decay from relatively high stress to relatively low stress is much quicker than in the 0.1 case, where the decay is much more gradual. Furthermore, as this behaviour is dependent on the relative difference in ratios, changing the absolute size of the samples has no impact, as long as the interfacing geometries of the inertial masses and end washers are also changed accordingly.

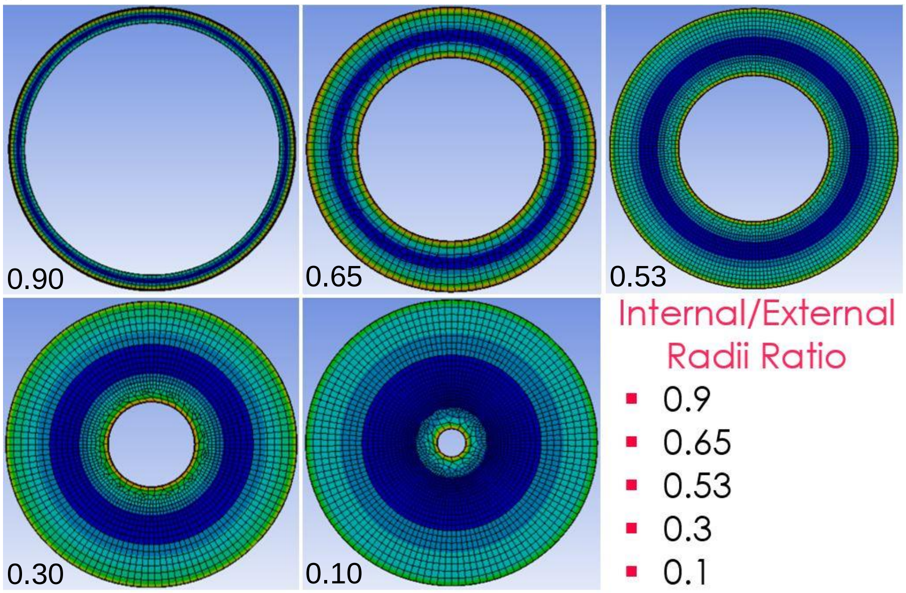

Figure 8: Radii Ratio Study - Rubber

3.4 Material Boundaries Study

The significant difference in stress distributions observed between the mild steel and rubber samples prompted the investigation of the impact that material properties have on gripping. Figure 9 adds Nylon’s stress distribution alongside the mild steel and rubber samples. By doing so, a step change in stress distribution from the mild steel to nylon to rubber is observed.

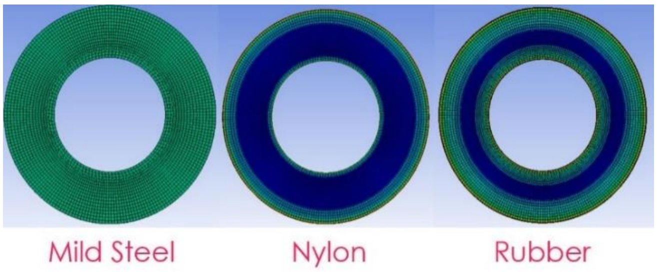

Figure 9: Stress Distribution Across Materials

To better understand this behaviour, a “sandbox” material was defined in the simulation environment. This allows for the tuning of one property variable at a time, which enables direct corollary tracking of stress distribution. A sandbox material which mirrored mild steel's properties was defined. Next, just the Young's modulus of the sandbox material is gradually adjusted to observe changes in the stress distribution. It is important to note that the properties of the rest of the rig stay constant throughout all testing and the ideal IR/ER ratio sample dimensions for a mild steel sample are used. Figure 10 begins to highlight the importance of material properties. As Young's modulus is gradually decreased from 220GPa to 2.2 GPa and 22MPa, i.e. changing two orders of magnitude each time, the stress distribution shifts from being uniform to being more concentrated on the external edges. The 22MPa test shows limited stress on the inside edge, however the majority of the stress is still largely on the external edge. This behaviour expectedly matches the variation seen in Figure 8 and partially mirrors the low IR/ER cases of the radii ratio study, where the external edges become well gripped. Notably also, if the surrounding beam and inertial masses are changed to match the properties of the sandbox material, the uniform stress distribution seen in the 220GPa case is reproduced. This suggests that the stress distribution observed is dependent on the relative Young's modulus boundary between the material and the rest of the test rig.

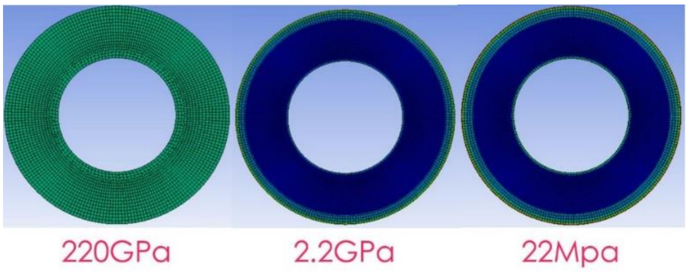

Figure 10: Sandbox Materials - Young's Modulus Variation

3.5 Verifying Gripping Integrity

It was important to verify that the test rig design changes described above yielded a gripping profile sufficient to preclude sample slipping. The possibility of slipping was therefore checked when using the rigs to determine material properties. This was done by using a logarithmic linearity check, where the gradient of the absolute acceleration time history curve is evaluated on a logarithmic plot. A linear system displays a straight-line gradient and non-linear systems, due to their slippage and friction, display some curvature in the gradient.

The top pair of images in Figure 11 shows a typical measured response for the rigs developed and the characteristic exponential decay curve is verified by the straight-line gradient of the linearity check. By comparison, the bottom pair of images show one of the non-linear modes found in an alternative rig design, with varying acceleration decay rates, and a much more inconsistent gradient on the linearity check. This alternative rig demonstrated significant gapping behaviour, even rattling during testing. Notably, this behaviour is broadly consistent across material samples and results for steel samples are presented. Critically for the proposed test setup, the behaviour observed shows that the test operates in the linear regime throughout the frequency range of interest, at least for the range of amplitudes tested. Furthermore, when updating the finite element model and extracting Young's modulus, non-linear contact definitions are not required, and the preload used is sufficient.

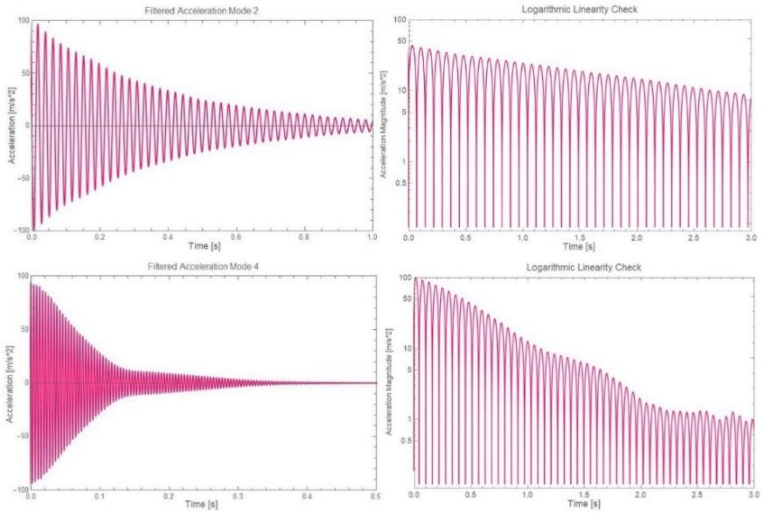

Figure 11: Time History Linearity Check

4 Experimental Methodology

The test method employs a hybrid approach, utilising both experimental and simulation techniques. Experimental modal analysis methods were used to excite vibration. Here an instrumented hammer is used to excite the bending modes of the beam and an accelerometer, bolted firmly onto the beam, records the system's dynamic response. This yields force and acceleration time histories for the beam system during vibration.

The Fourier transform of the acceleration response is divided by the Fourier transform of the impact force to produce a spectrum of the frequency response function of the system. Resonant modes appear as peaks on the spectrum and their frequencies are recorded as modal natural frequencies. A finite element model of the system was constructed in which the modulus of elasticity of the material samples can be tuned. This enables the simulated modal natural frequencies to be matched with those derived from the experiment. Thus, tracking of variations in modulus of elasticity of the sample with respect to frequency is achieved. It should be noted that mesh convergence analysis was conducted on the simulation to ensure reliability. Further, calibration using samples made from the same material as the rest of the rig (mild steel) was conducted. This can be used to compensate for changes in the rig's material properties with frequency, as even the mild steel displays very small changes in Young's modulus.

To find the damping ratio of a material sample, two methods are employed. Firstly, the time history is reversed and then filtered to remove noise. The resulting decay is then curve fitted with a mathematical damping model to produce damping ratio [26]. Secondly, each resonance peak in the spectrum is curve fitted with a mathematical resonance model to yield a damping ratio – the standard circle fitting procedure is applied. This approach produces two measurements of damping ratio, which are used to cross-validate results. However, this is the damping ratio of the entire setup and not the material samples themselves. Thus, the results produced are useful for relative property comparison, but are difficult to compare with alternative testing methods. Hence, a method of factoring out the influence of the surrounding setup is required.

4.1 Specific Damping Factor

A new approach to measuring damping is introduced, one which allows for the isolation of measured damping resulting from the just the material. This is derived from considering that fundamentally, material damping is a ratio between the energy dissipated by, and the energy stored in, a material.

$$Material\ Damping = \frac{Energy\ Dissipated\ Per\ Cycle}{Maximum\ Energy\ Stored}\ (Eq. 1)$$

A spring, mass and damper model is useful to consider as the energy dissipated from a material may be modelled as the energy dissipated by a damper and the energy stored may be modelled as the energy stored in a spring. The energy dissipated by a damper may be obtained by integrating the work done by it. Importantly however, this is the average energy dissipated per cycle. Additionally, the energy stored in a spring is the instantaneous energy at maximum strain. Thus, to obtain equivalent quantities, the energy dissipated by the damper needs to be multiplied by the time period, as shown in equation 2:

$$\frac{Energy\ Dissipated\ Per\ Cycle}{Maximum\ Total\ Strain\ Energy\ Stored} = \frac{\frac{1}{2}cv^2T}{\frac{1}{2}kx^2}\ \ (Eq. 2)$$

Simplifying and putting in terms of damping ratio (ζ), results in material damping being equal to 4ζπ. This is sufficient for a system with just the material sample. However, as material characterisation methods have surrounding components to support and grip the samples or measure response, the influence of the rest of the rig must be factored out. To achieve that, a harmonic response simulation is used, which enables potential energies throughout the test rig to be determined. The ratio between energy stored in the samples and energy stored in the rest of the rig is then computed for every mode. With this, the measured damping ratio from both measurement methods is scaled to determine the contribution of the material sample to the overall measured damping.

Mathematically this may be represented as equation 3:

$$Specific\ Damping\ Factor = \frac{4\zeta\pi \times Total\ System\ Energy\ Stored}{Energy\ Stored\ in\ Samples}\ (Eq. 3)$$

This allows for separation of the material sample’s damping characteristics, as opposed to the overall damping properties of the test rig. This is an evolution from the previously proposed specific damping capacity and loss factor approaches [27], as here, the focus is on separating the potential energy stored in the sample and the remainder of the test rig. Existing methods measure energy dissipated by the entire test rig, whereas in the proposed method, energy stored in different parts of the setup is calculated using simulation.

4.2 Validation

Validation for the method was achieved via three distinct approaches. Firstly, a previous iteration of the test method which used rectangular samples and inertial masses, along with a different dimension beam, can be compared to the presented test setup. Using two independent methods of characterisation and comparing the results has the added benefit of providing more data points within the frequency range. This is due to the change in beam dimensions which yields an altered frequency distribution for the modes. Secondly, the observed results are compared with existing databases to check the precision of results. Finally, a viscoelastic material, Sorbothane, is characterised using the presented approach and compared with manufacturer evaluation methods.

Four testing campaigns have been conducted, two using the rectangular samples setup, and two using the circular samples setup. Each campaign involves performing ten hammer hit runs, from which the best three runs are selected. This selection is done so on the basis of minimising double-hits and thus improving time history clarity. A double, or multiple hit run occurs when the hammer imparts multiple impacts into the structure, and although this is factored out when calculating the frequency response function, it still may add noise into the spectrum. Natural frequency and damping ratio values are then extracted from these three selected runs and averaged to account for run-to-run variability.

Impact excitation from a modal hammer is ideal as the ring-down is only due to the response of the test article. If a shaker were to be used, although it may offer more repeatable force excitation, the adverse impact of the shaker-structure interactions would be very difficult to decouple. It is important to add that only bending modes are investigated as this makes each mode easier to identify. Given the simple geometry of test setup, the finite element model constructed is accurate in predicting which modes are indeed bending as opposed to torsional or longitudinal.

Four typical materials ranging from mild steel and nylon 6, to two different types of rubbers have been characterised using both experimental setups. The rubbers are commonly found industrial damping material with different shore hardness values. Sorbothane is also tested and compared with the manufacturer's supplied data sheet. This range of testing was conducted to enable validation of the test setup and method across multiple material families.

5 Results

The primary objective of developing the method is to significantly extend the frequency range that materials may be accurately characterized in. To that end, a large number of modes must be present to sufficiently characterise the frequency range. Further the mode natural frequencies must be uniformly spread through the test range. Figure 12 shows the range of frequencies and the associated number of bending modes observed. This demonstrates that the modes of the test setup are sufficient to observe trends and capture variation in properties, up to at least 2000Hz.

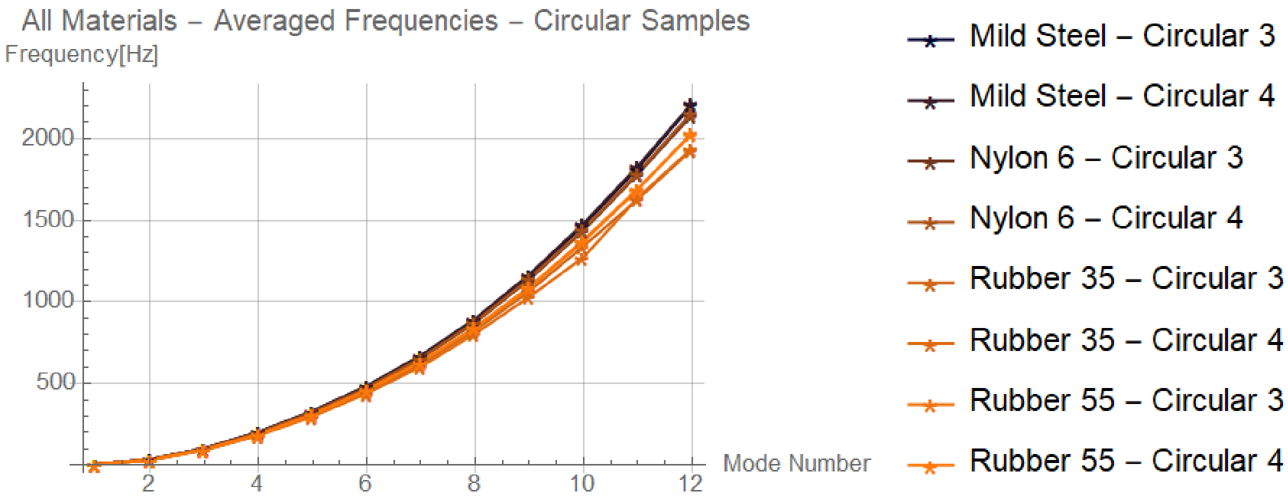

Figure 12: Bending Mode Distribution in Frequency Range

The modulus of elasticity variation with frequency is captured for each of the four material samples and is compared between both versions of the test setup. The first graph in figure 13 shows the grouping between the two rigs and portrays variations within the same testing method. Variation between campaigns using the same rig is minimal, consistently being below 1% for steel with a maximum of 1.9%, thereby reinforcing the repeatability of the method. This is especially encouraging as this behaviour holds true for the higher frequencies. Further, observing the potential energy stored in the sample at each mode also demonstrated that sample excitation was relatively uniform throughout the frequency range. Thus, there is no natural frequency where the results must be ignored because the sample is insufficiently exercised. As a result, the method is valid at each natural frequency throughout the test range.

Nylon 6 shows the largest variation in modulus of elasticity with the same rig with the rubbers being more tightly grouped. Despite this, the measured results fall within the range of values outlined in the manufacturer's data sheet [28], [29]. For example, the stiffer of the two nylon 6 samples tested, the test setup measured values average to 3.9GPa over the frequency range, while the data sheet quotes a modulus of elasticity of 3.3 GPa, but as a static value. Similarly, the softer of the two nylon 6 samples quotes a modulus of elasticity of 1.7GPa, and the measured value from the test setup is 1.9GPa over the full frequency range.

As the exact alloy of mild steel and composition of rubber is unknown, more general comparison to their respective material categories were made [30], [31]. As the variation in Young's modulus over the frequency range was less significant with these materials, better agreement with material library ranges was achieved. Despite this, the variation between the rectangular and circular rigs is more pronounced, likely owing to differences in sample quality, machining or loading. These factors are difficult to recreate in the simulation and represents error arising from the equipment. Yet, both rigs, with differing samples and geometries, are able to produce similar results which suggests that the method itself produces reproducible results.

The second graph in figure 13 effectively demonstrates the need to consider damping with a more detailed analysis than just damping ratio. Rubber, as expected, has larger damping compared to steel, and, although the data shows this accurately for the higher frequencies, there is apparently very little difference in damping at lower frequencies. This shows that the measured damping ratio is not the correct approach when determining damping properties. The problem is the varying modal excitation that occurs between materials which is not captured with just damping ratio measurement. Further, using damping ratio makes tracking variation between test rigs difficult.

The specific damping approach converts the measured damping ratio into a more comparable material property as shown in the graphs in figure 14. At this point, it becomes prudent to note that both methods of damping ratio measurement (reverse filter fitting and mode fitting) yielded near identical results, as is demonstrated by the similarity of the specific damping factor graphs. Further, values of damping ratio are similar to results in the literature [32], but direct comparison is fruitless, given the difference in test setups.

Examination of damping using the energy stored and dissipated in the samples, compared to the rest of the test setup, differentiates between the materials in an intuitive manner. A high value for specific damping factor indicates a low proportion of energy stored in the sample. Thus, energy remains in the rest of the system and damping is low. In the case of rubber, more energy is transferred into the sample, thereby confirming the higher expected damping properties. For clarity, the amount of potential/strain energy stored within a material, in a given vibration cycle, corresponds to the amount of heat energy dissipated in the next cycle. Thus, the rubber which stores more per cycle also dissipates more overall, when compared to the polymers and steels.

The results indicate that the damping ability of a material all increase with frequency, with the stiffer materials showing the largest change. The magnitude of the change is notable as the results are plotted on a logarithmic plot. Over this frequency range, the damping ability of mild steel and nylon 6 increases by an entire order of magnitude. Rubber 35 experiences a similar but smaller increase, with rubber 55 being the most stable of the materials tested. Variation between campaigns and rigs remains small with rubbers but having greater disparities in the steel at low frequencies.

Figure 15 compares values for Sorbothane's dynamic Young's modulus as characterised using the proposed method, with values from the manufacturer. A high frequency DMA machine was used by the manufacturer for these values and testing was done on three types of Sorbothane, differentiated by their shore hardness rating (30, 50 and 70). The shore hardness of the Sorbothane characterised using the present method is unknown. Despite this, the measured values fall well within the range of manufacturer expected values [33] and correlates closely with Sorbothane 50. Hence the method appears promising in its ability to produce values that fall within manufacturer's values when contemporary characterisation approaches are used. As no values in literature were found that extended the manufacturer's 300Hz maximum frequency, comparison of Young's modulus to the full 2000Hz range of the method is not possible. Despite this, the method appears promising in its ability to produce similar results when compared to DMA, while extending the frequency range from 300Hz to 2000Hz and beyond. Important to note also is that the beam dimensions were optimised for the extended frequency range of 2000Hz. In cases where a greater number of modes are required only up to 300Hz, in order to achieve a greater resolution, a thinner/longer beam made from a less stiff material may be used.

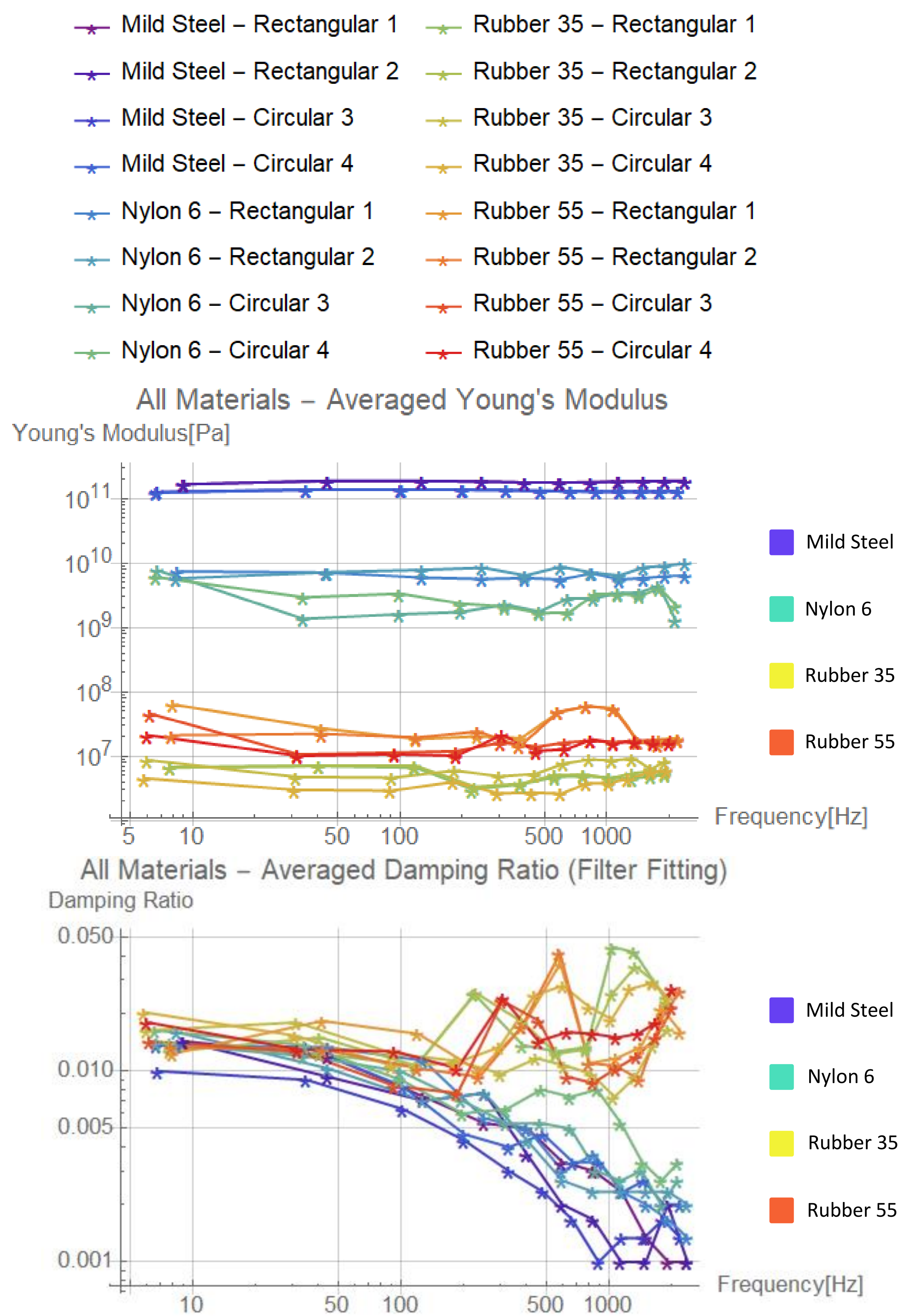

Figure 13: Modulus of Elasticity & Damping Ratio Variation with Frequency

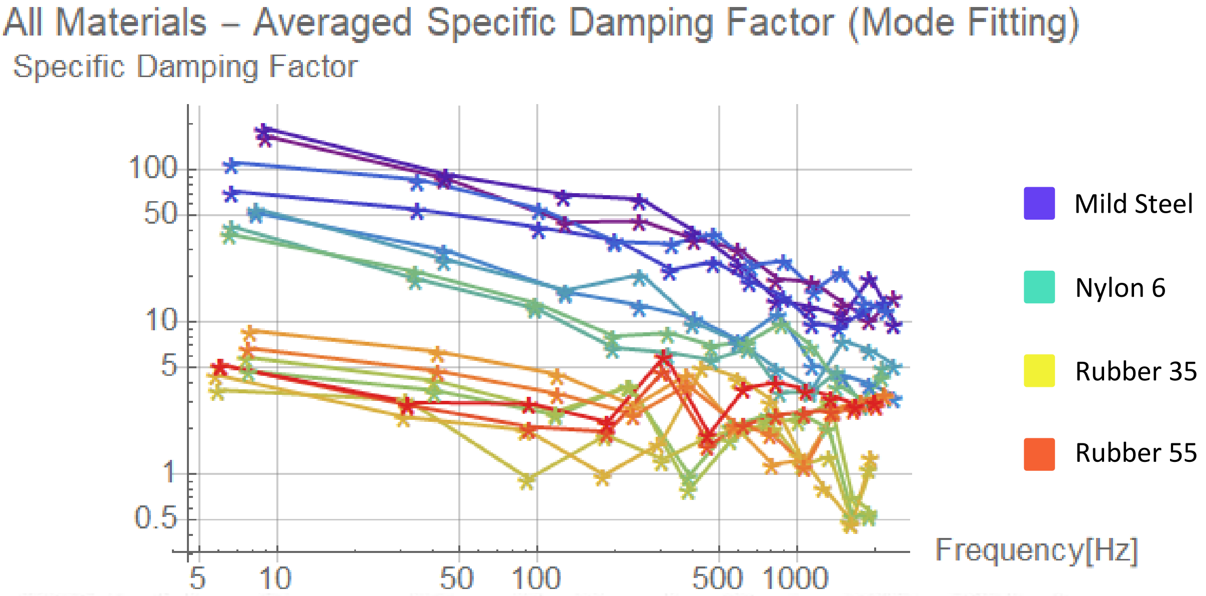

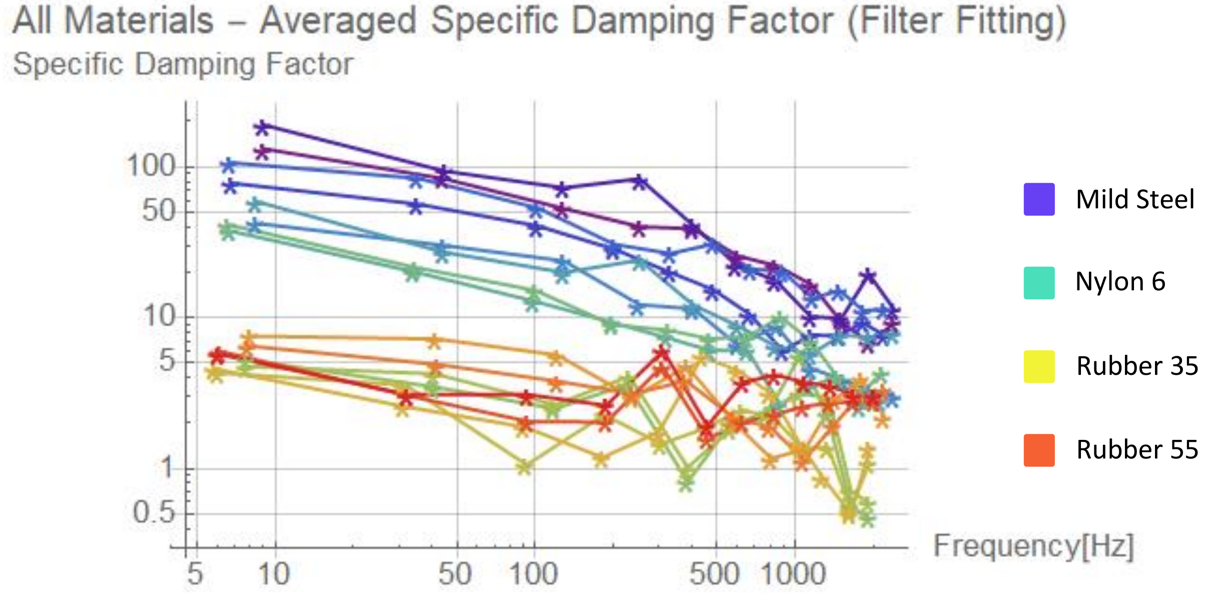

Figure 14: Specific Damping Factor Variation with Frequency

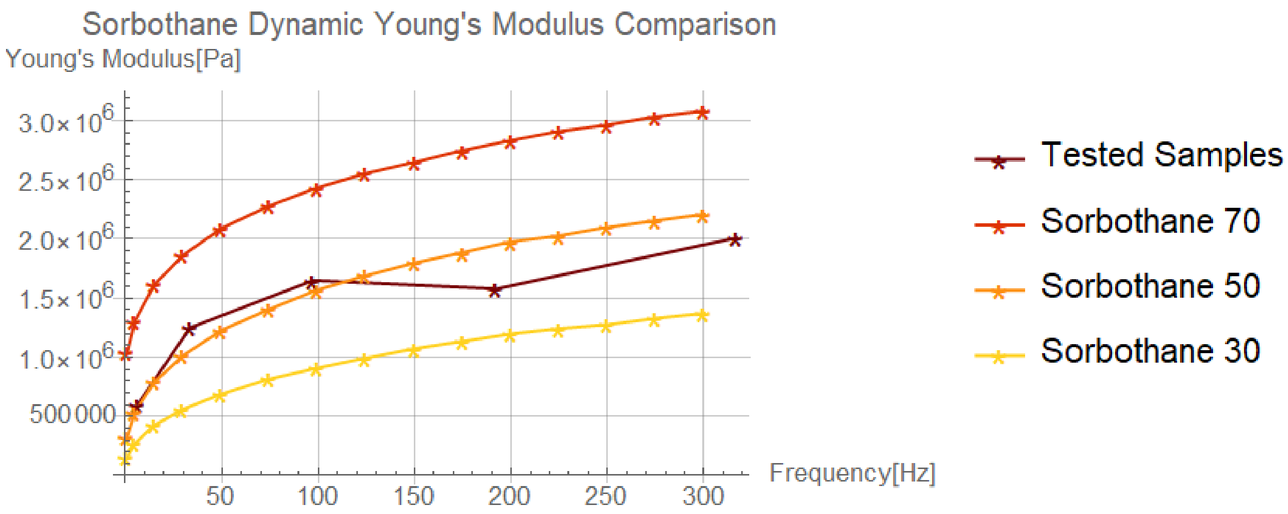

Figure 15: Sorbothane Dynamic Young's Modulus Characterisation & Comparison

4 Scope & Discussion

Evaluating the precision of the rig proves to be difficult as a result of the hybrid, experimental-simulation approach and not knowing the exact composition of materials. Steps that have been taken to ensure sources of error are minimised include: sample design, equipment calibration, multiple data runs per campaign, mesh quality and simulation accuracy. Further work is required using samples where the exact composition is known in order to evaluate the precision of the method.

One limitation of the method is the stiffness of the test setup. The modulus of elasticity of the samples must be below that of the material used to construct the rig as otherwise, the simulation tuning is ineffective. However, if required, this limitation may be rectified by making the rig out of a stiffer material. The setup is also compatible with temperature testing and an oven and freezer are presently being used to do so. This method is sufficiently simple that in-house methods for measurement are possible, and no specialist training is required.

The main output of this method is that it enables accurate and quick material simulation. Current simulation methods rely on accurate damping ratio values across a specified frequency range. Material characterisation this thorough is often beyond the scope for some projects, which leads to estimations from generalised data sources being made.

Using the proposed specific damping factor opens a new avenue in the finite element simulation of damping. Having evaluated the undamped mode shapes of a system, the strain energy in each member of the undamped structure can be used to calculate the damping ratio for each mode. This streamlines simulation damping modelling by removing the need to estimate damping ratios or use results from literature where the influence of the setup is not accounted for. Instead, the specific damping factor of a material can be recorded over a large frequency range, such that damping ratio that is correct for any particular setup, is calculated.

7 Conclusion

A novel material characterisation method has been presented that employs a quasi-cantilever beam setup to excite vibrational modes which exercise material samples. Test data from experiments was combined with finite element simulation to produce modulus of elasticity and damping properties.

- Variation in modulus of elasticity and damping properties was tracked over a wide frequency range (2-2000Hz).
- Gripping test samples is always a significant challenge. This was addressed by finite element design of sample shapes, and sharp-edged circular discs with a central hole were selected.
- Four materials with differing properties have been tested successfully.
- Comparison between two rig designs and characterisation of a standard damping material has demonstrated the accuracy of the method.
- An evolution of existing damping descriptions is also presented which is superior to just using damping ratios.
- The need for estimating damping ratio in simulation can be eliminated by using specific damping factor and simulated undamped mode shapes to calculate application specific damping ratios.
- The full test and simulation methodology is designed to be easy to operate and requires little specialist training.
- The setup itself is simple to manufacture and the modularity of the design yields great flexibility in characterising narrow or wide frequency ranges.

Overall, this method proves to be a quick, inexpensive and promising way to characterise dynamic material properties and encourages rapid material prototyping in engineering design and simulation.

References

[1] J. Bachmann, C. Hidalgo and S. Bricout, "Environmental analysis of innovative sustainable composites with potential use in aviation sector—A life cycle assessment review," Science China Technological Sciences, 2017.

[2] Johnson Matthey, "The Importance Of Characterisation Techniques," 2016.

[3] R. Chartoff, J. Menczel and S. Dillman, "Dynamic Mechanical Analysis (DMA)," in Thermal Analysis of Polymers, 2009.

[4] W. Broughton, "6 - Testing the mechanical, thermal and chemical properties of adhesives for marine environments," Adhesives in Marine Engineering, pp. 99-154, 2012.

[5] Metravib, "VHF 104 - Very High Frequencies Analyzer," 2015.

[6] S. Ackermann, "Generating a Master Curve Using Dynamic Mechanical Analysis (DMA)," 23 April 2024. [Online]. Available: https://ctherm.com/resources/newsroom/blog/generating-a-master-curve-using-dma/.

[7] D. I. Jones, Handbook of viscoelastic vibration damping, John Wiley & Sons., 2001.

[8] B. Khandelwal, C. Wijesinghe and S. Sriraman, "Effect of Alternative Fuels on Emissions and Engine Compatibility.," in Energy for Propulsion, Green Energy and Technology, 2018, pp. 27-50.

[9] H. Goyder, "Natural Frequencies and Damping of a Full-Scale Pipe Loop in Air and Water," in ASME 2017 Pressure Vessels and Piping Conference., 2017.

[10] H. Mevada and D. Patel, "Experimental Determination of Structural Damping of Different Materials.," in Procedia Engineering, 2016.

[11] P. Kulkarni, A. Bhattacharjee and B. K. Nanda, "Study of damping in composite beams.," in International Conference on Emerging Trends in Materials and Manufacturing Engineering, 2018.

[12] M. Mohammadali and H. Ahmadian, "Improvement in Modal Testing Measurements by Modeling and Identification of Shaker–Stinger–Structure Interactions.," Experimental Techniques, vol. 40, pp. 49-57, 2016.

[13] A. V. Sergueeva, J. Zhou, B. E. Meacham and D. J. Branagan, "Gage length and sample size effect on measured properties during tensile testing.," Materials Science and Engineering A, vol. 526(1–2), p. 79–83, 2009.

[14] R. F. Gibson, "Modal vibration response measurements for characterization of composite materials and structures.," Composites Science and Technology, , vol. 60, no. 15, p. 2769–2780, 2000.

[15] Zwick, & Roell, "Testing Systems The specimen under control - Specimen grips and test tools Intelligent Testing.," [Online]. Available: https://www.zwickroell.com/fileadmin/content/Files/SharePoint/user_upload/Brochures_EN/04_745_Specimen_grips_and_test_tools_FP_EN.pdf. [Accessed April 2021].

[16] Anton Paar, "How to Prevent Sample Slip in Tensile DMA Measurements. User Manual Anton Paar.," [Online]. [Accessed 2019].

[17] A. Mucsi, "Analysis of Stress Distribution in Tensile Test Specimens Using Modified Versions of a Novel Gripping System. Universal Journal of Mechanical Engineering," Universal Journal of Mechanical Engineering, vol. 1, no. 4, p. 109–113, 2013.

[18] A. Anssari-Benam, K. Legerlotz and D. L. Bad, "On the specimen length dependency of tensile mechanical properties in soft tissues: Gripping effects and the characteristic decay length," Journal of biomechanics, pp. 2481-2482, 2012.

[19] A. E. H. Love , A treatise on the mathematical theory of elasticity, Dover Publications, 1944.

[20] R. A. Toupin, " Saint-Venant's Principle," Archive for Rational Mechanics and Analysis, 1965.

[21] H. Sönnerlind, "Applying And Interpreting Saint Venant's Principle," Cosmol, 22 January 2018. [Online]. Available: https://www.comsol.com/blogs/applying-and-interpreting-saint-venants-principle. [Accessed September 2020].

[22] I. Choi and C. Horgan, "Saint-Venant's Principle and End Effects in Anisotropic Elasticity," Journal of Applied Mechanics, 1977.

[23] I. Chowdhury and S. Dasgupta, "Computation of Rayleigh Damping Coefficients for Large Systems,"

Electronic Journal of Geotechnical Engineering, vol. 43, pp. 6855-6868, 2003.

[24] C. Cruz and E. Miranda, "A Critical Review of the Rayleigh Damping Model.," in 6th World Conference on Earthquake Engineering, 2017.

[25] R. Pijpers and H. Slot, "Friction coefficients for steel to steel contact surfaces in air and seawater," May 2021. [Online]. Available: https://www.sintef.no/globalassets/project/eera-deepwind-2020/posters/poster_richard-pijpers.pdf.

[26] G. Hugh, L. Damien, P. Ind and D. Brown, "Friction and damping associated with bolted joints: results and signal processing.," in Proceedings of the ISMA 2016 International Conference on Noise and Vibration Engineering, 2016.

[27] E. Sarlin, Y. Liu, M. Vippola, M. Zogg, P. Ermanni, J. Vuorinen and T. Lepistö, "Vibration damping properties of steel/rubber/composite hybrid structures," Composite Structures, vol. 94, p. 3327–3335, 2012.

[28] Direct Plastics, "Nylon Extruded 6," April 2021. [Online]. Available: https://www.directplastics.co.uk/pdf/datasheets/Nylon%20Extruded%206%20Black%20Data%20Sheet.pdf.

[29] Plastim, "Nylon 6 Extruded," January 2015. [Online]. Available: https://plastim.co.uk/wp-content/uploads/2019/07/Nylon-6-Extruded-Natural-Technical-Data-Sheet.pdf.

[30] Mat Web, "Mild Steels, General Properties," April 2021. [Online]. Available: https://www.matweb.com/search/datasheet.aspx?bassnum=MS0001&ckck=1.

[31] Bestech, "Modulus Of Elasticity - Young's Modulus For Some Common Materials," April 2021. [Online]. Available: https://www.bestech.com.au/wp-content/uploads/Modulus-of-Elasticity.pdf.

[32] F. Orban, "Damping of materials and members in structures," in 5th International Workshop on Multi-Rate Processes and Hysteresis, 2010.

[33] Sorbothane, "Data Sheet," 17 August 2021. [Online]. Available: https://www.sorbothane.com/wp-content/uploads/101-sorbothane-material-properties.pdf.